



Off the Baryonic Tully–Fisher Relation: A Population of Baryon-dominated Ultra-diffuse Galaxies

Pavel E. Mancera Piña^{1,2}, Filippo Fraternali¹, Elizabeth A. K. Adams^{1,2}, Antonino Marasco^{1,2}, Tom Oosterloo^{1,2}, Kyle A. Oman¹, Lukas Leisman³, Enrico M. di Teodoro⁴, Lorenzo Posti⁵, Michael Battipaglia³, John M. Cannon⁶, Lexi Gault³, Martha P. Haynes⁷, Steven Janowiecki⁸, Elizabeth McAllan³, Hannah J. Pagel⁹, Kameron Reiter³, Katherine L. Rhode⁹, John J. Salzer⁹, and Nicholas J. Smith⁹

¹ Kapteyn Astronomical Institute, University of Groningen, Landleven 12, 9747 AD, Groningen, The Netherlands; pavel@astro.rug.nl

² ASTRON, Netherlands Institute for Radio Astronomy, Postbus 2, 7900 AA Dwingeloo, The Netherlands

³ Department of Physics and Astronomy, Valparaiso University, 1610 Campus Drive East, Valparaiso, IN 46383, USA

⁴ Research School of Astronomy and Astrophysics, The Australian National University, Canberra, ACT 2611, Australia

⁵ Université de Strasbourg, CNRS UMR 7550, Observatoire astronomique de Strasbourg, 11 rue de l'Université, F-67000 Strasbourg, France

⁶ Department of Physics & Astronomy, Macalester College, 1600 Grand Avenue, Saint Paul, MN 55105, USA

⁷ Cornell Center for Astrophysics and Planetary Science, Space Sciences Building, Cornell University, Ithaca, NY 14853, USA

⁸ University of Texas, Hobby-Eberly Telescope, McDonald Observatory, TX 79734, USA

⁹ Department of Astronomy, Indiana University, 727 East Third Street, Bloomington, IN 47405, USA

Received 2019 July 8; revised 2019 August 26; accepted 2019 September 1; published 2019 September 25

Abstract

We study the gas kinematics traced by the 21 cm emission of a sample of six HI-rich low surface brightness galaxies classified as ultra-diffuse galaxies (UDGs). Using the 3D kinematic modeling code ^{3D}Barolo we derive robust circular velocities, revealing a startling feature: HI-rich UDGs are clear outliers from the baryonic Tully–Fisher relation, with circular velocities much lower than galaxies with similar baryonic mass. Notably, the baryon fraction of our UDG sample is consistent with the cosmological value: these UDGs are compatible with having no “missing baryons” within their virial radii. Moreover, the gravitational potential provided by the baryons is sufficient to account for the amplitude of the rotation curve out to the outermost measured point, contrary to other galaxies with similar circular velocities. We speculate that any formation scenario for these objects will require very inefficient feedback and a broad diversity in their inner dark matter content.

Unified Astronomy Thesaurus concepts: Dwarf galaxies (416); Galaxy formation (595); Galaxy evolution (594); Galaxy kinematics (602); Galaxy dynamics (591); Dark matter (353); Low surface brightness galaxies (940); Galaxy rotation curves (619)

1. Introduction

The baryonic Tully–Fisher relation (BTFR; McGaugh et al. 2000; McGaugh 2005) is a tight sequence in the baryonic mass–circular velocity plane followed by galaxies of different types (e.g., den Heijer et al. 2015; Lelli et al. 2016a; Ponomareva et al. 2017). It has been of paramount importance and widely used for calibrating distances to extragalactic objects and to constrain, for example, semianalytical and numerical models of galaxy formation and evolution (e.g., Governato et al. 2007; Dutton 2012; McGaugh 2012; Sales et al. 2017 and references therein).

Among the galaxies populating the BTFR, low surface brightness (LSB) galaxies are of particular interest, and have been used to investigate the mass distribution and stellar feedback processes at dwarf galaxy scales (e.g., Zwaan et al. 1995; Dalcanton et al. 1997; de Blok 1997; Di Cintio et al. 2019).

Ultra-diffuse galaxies (UDGs; van Dokkum et al. 2015) are an especially notable subset of the LSB galaxy population due to their extremely low surface brightness values while having effective radii comparable to L^* galaxies. While these galaxies have been known for decades (e.g., Sandage & Binggeli 1984; Impey et al. 1988), their recent detection in large numbers in different galaxy clusters, groups, and even in isolated environments (e.g., Leisman et al. 2017; Román & Trujillo 2017; Mancera Piña et al. 2019) has sparked a renewed interest in them.

Many UDGs in isolation are HI-rich, opening the possibility of investigating their gas kinematics. The most systematic study of HI in UDGs has been carried out by Leisman et al. (2017), who studied 115 sources¹⁰ from the Arecibo Legacy Fast Arecibo L-band Feed Array (ALFALFA) catalog (Giovanelli et al. 2005), as well as a small subsample of three sources with interferometric HI data, that meet the optical criteria of having $R_c \geq 1.5$ kpc and $\langle \mu(r, R_c) \rangle \geq 24$ mag arcsec⁻², according to Sloan Digital Sky Survey photometry. The authors reported that such galaxies are HI-rich for their stellar masses and have low star formation efficiencies, similar to other gas-dominated dwarfs (e.g., Geha et al. 2006). Perhaps most intriguing, Leisman et al. (2017) reported that the velocity widths (W_{50}) of the global HI profiles of their UDGs were significantly narrower than in other ALFALFA galaxies with similar HI masses. However, without resolved HI imaging of a significant sample, this result could be attributed to a very strong inclination selection effect for their sample, or systematics when deriving W_{50} .

Taking all of the above as a starting point, in this work we undertake 3D kinematical modeling of resolved HI synthesis data to study the gas kinematics of six HI-rich UDGs. The rest of this Letter is organized as follows: in Section 2 we introduce our sample of galaxies with their main properties and we describe our strategy for deriving their kinematics. We present

¹⁰ HI-rich UDGs represent $\sim 6\%$ of all galaxies with $M_{HI} \sim 10^{8.8} M_\odot$, with a cosmic abundance similar to cluster UDGs (Jones et al. 2018; Mancera Piña et al. 2018).

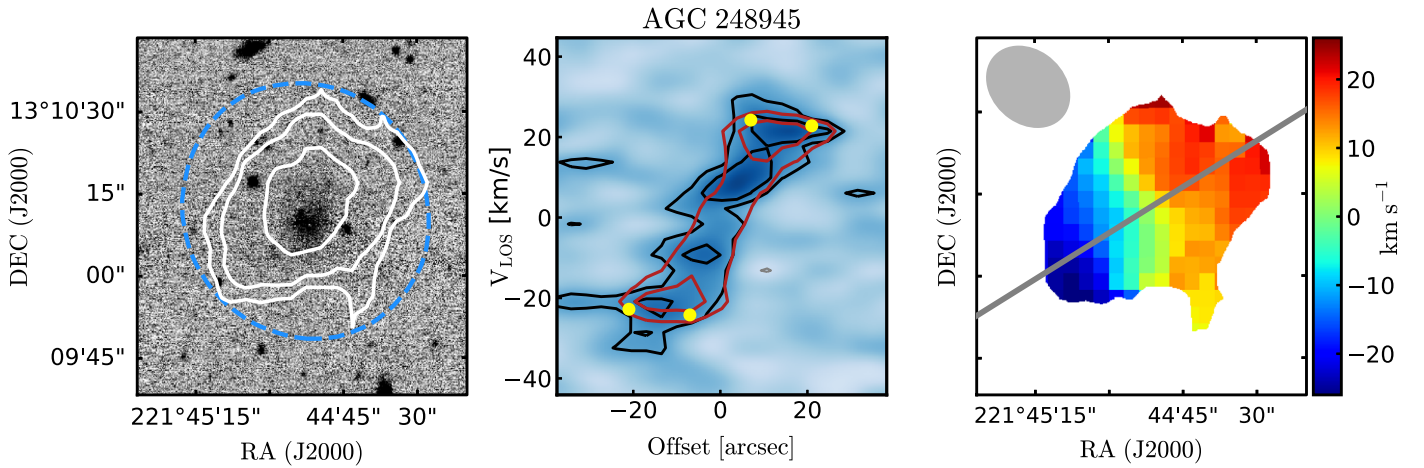


Figure 1. A representative galaxy from our sample, AGC 248945. Left: H I contours on top of the r -band image; the contours are at 0.88 , 1.76 , and 3.52×10^{20} H I atoms per cm^2 , the outermost contour corresponds to $S/N \approx 3$. The blue ellipse shows the inclination the galaxy would need to be in the BTFR (see the text for details). Middle: PV diagram along the kinematic major axis; black and red contours correspond to data and ^3D Barolo best-fit model, respectively; the yellow points show the recovered rotation velocities. Right: observed velocity field, at the same scale as the left panel. The gray line shows the kinematic major axis, and the gray ellipse the beam.

Table 1

Name, Distance, Inclination, Baryonic Mass, Gas-to-stellar Mass Ratio, Circular Velocity, Central Surface Brightness, and Color of Our Sample

Name	Distance (Mpc)	Inclination (deg)	$\log(M_{\text{bar}}/M_{\odot})$	M_{gas}/M_{\star}	V_{circ} (km s^{-1})	$\mu(g,0)$ (mag arcsec^{-2})	$g-r$ (mag)
AGC 114905	76	33	9.21 ± 0.20	$7.1^{+4.9}_{-2.3}$	19^{+6}_{-4}	23.62 ± 0.13	0.30 ± 0.12
AGC 122966	90	34	9.21 ± 0.14	$29.1^{+11.9}_{-7.0}$	37^{+6}_{-5}	25.38 ± 0.23	-0.10 ± 0.22
AGC 219533	96	42	9.36 ± 0.27	$19.7^{+12.2}_{-8.8}$	37^{+5}_{-6}	24.07 ± 0.33	0.12 ± 0.12
AGC 248945	84	66	9.05 ± 0.20	$2.4^{+1.6}_{-0.8}$	27^{+3}_{-3}	23.32 ± 0.35	0.32 ± 0.11
AGC 334315	73	52	9.32 ± 0.14	$23.7^{+9.8}_{-5.9}$	26^{+4}_{-3}	24.52 ± 0.13	-0.08 ± 0.18
AGC 749290	97	39	9.17 ± 0.17	$6.1^{+2.9}_{-1.7}$	26^{+6}_{-6}	24.66 ± 0.30	0.17 ± 0.12

Note. Distances, taken from Leisman et al. (2017), have an uncertainty of ± 5 Mpc, while the uncertainty for the inclination is $\pm 5^{\circ}$. The central surface brightness is obtained from an exponential fit to the g -band surface brightness profile.

our results and discussion in Section 3, to then conclude in Section 4. Throughout this work we adopt a Λ CDM cosmology with $\Omega_{\text{m}} = 0.3$, $\Omega_{\Lambda} = 0.7$, and $H_0 = 70 \text{ km s}^{-1} \text{ Mpc}^{-1}$.

2. Sample and Kinematics

Our sample consists of six galaxies identified as H I-bearing UDGs by Leisman et al. (2017). They have $M_{\text{H I}} \sim 10^9 M_{\odot}$ and are relatively isolated, by requiring that any neighbor with measured redshift within $\pm 500 \text{ km s}^{-1}$ should be at least at 350 kpc away in projection. Moreover, they have $R_e > 2$ kpc, to ease optical follow-up.

Our observations were obtained with two interferometers: the data for AGC 122966 and AGC 334315 come from the Westerbork Synthesis Radio Telescope (program R13B/001; PI: Adams) and the rest from the Karl G. Jansky Very Large Array (programs 14B-243 and 17A-210; PI: Leisman). The observations and data reduction procedure are described in Leisman et al. (2017) and more details will be given in L. Gault et al. (2019, in preparation). Three more galaxies for which we have data are excluded from this analysis. AGC 238764 seems to have ordered rotation of about 20 km s^{-1} , but our data cube misses significant flux with respect to the ALFALFA detection. AGC 749251 shows hints of a velocity gradient but it is barely resolved and we are not able to constrain its inclination better than $i \lesssim 30^{\circ}$. AGC 748738 shows signs of a gradient in velocity, but the data are very noisy. We decide not to consider these three galaxies to keep a reliable

sample for the kinematic fitting, but more details on these sources will be given in L. Gault et al. (2019, in preparation).

We estimate the baryonic mass of our UDGs as $M_{\text{bar}} = 1.33 M_{\text{H I}} + M_{\star}$, with $M_{\text{H I}}$ given by

$$\frac{M_{\text{H I}}}{M_{\odot}} = 2.343 \times 10^5 \left(\frac{d}{\text{Mpc}} \right)^2 \left(\frac{F_{\text{H I}}}{\text{Jy km s}^{-1}} \right), \quad (1)$$

where we assume (Hubble flow) distances as listed in Leisman et al. (2017), and fluxes derived from the total H I-maps using the task FLUX from GIPSY (Vogelaar & Terlouw 2001).

Stellar masses are obtained from the mass-to-light ratio–color relation of Herrmann et al. (2016) for an absolute magnitude in the g band and a $(g-r)$ color. In order to derive such measurements we perform aperture photometry following the procedure described in Marasco et al. (2019) on deep optical data, obtained with the One Degree Imager of the WIYN 3.5 m telescope at the Kitt Peak National Observatory (Leisman et al. 2017; L. Gault et al. 2019, in preparation).

We find a mean $M_{\text{H I}}/M_{\star} \approx 15$, confirming that the baryonic budget is mainly set by the H I content, which we can robustly measure. Table 1 gives the name, distance, inclination, baryonic mass, gas-to-stellar mass ratio, circular velocity, central surface brightness, and color of our galaxies. Figure 1 shows the stellar image, zeroth-moment map, major-axis position–velocity (PV) diagram, and observed velocity field

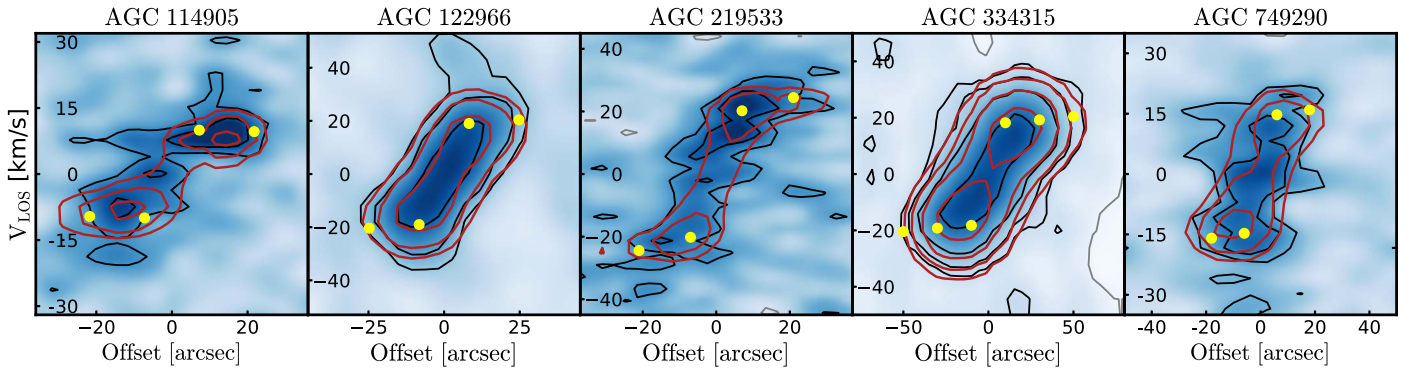


Figure 2. PV slices along the major axes of our galaxies. Contours and points as in Figure 1, where AGC 248945 is shown. The narrowness of the PV diagrams suggests low gas velocity dispersions, as confirmed by ${}^3\text{DBarolo}$.

for a representative case, AGC 248945. Figure 2 shows the PV diagrams for the rest of our sample.

Rotation velocities are derived with the software ${}^3\text{DBarolo}$ ¹¹ (Di Teodoro & Fraternali 2015), which fits tilted-ring disk models to the HI data cubes (e.g., Iorio et al. 2017; Bacchini et al. 2019). This approach is particularly suited to deal with our low spatial resolution data (2–3 resolution elements per galaxy side) as it is virtually unaffected by beam-smearing (e.g., Di Teodoro et al. 2016). While further details about the properties of our sample and the configuration used in ${}^3\text{DBarolo}$ will be given in P. E. Mancera Piña et al. (2019, in preparation), here we briefly summarize our methodology.

We give the position angle and inclination of the galaxies to ${}^3\text{DBarolo}$. For the former we choose the angle that maximizes the amplitude of the PV slice along the major axis. The inclination of each galaxy is derived by minimizing the residuals between its observed zeroth-moment map and the zeroth-moment map of models of the same galaxy projected at different inclinations between 10° and 80° . We have tested this method blindly, without a priori knowledge of the position angle, inclination, or rotation velocity, on a sample of 32 HI-rich dwarfs drawn from the APOSTLE cosmological hydrodynamical simulations (Fattahi et al. 2016; Sawala et al. 2016), from which mock data cubes have been produced at resolution and signal-to-noise ratio (S/N) matching our observations, using the MARTINI software¹² (Oman et al. 2019). We find that we can consistently recover the position angle within $\pm 8^\circ$ and the inclination within $\pm 5^\circ$ as long as $i \gtrsim 30^\circ$, with no systematic trends. These small uncertainties in position angle and inclination have no significant impact on the recovered rotation velocities.

We run ${}^3\text{DBarolo}$ with fixed inclination and position angle, and the rotation velocity and velocity dispersion as free parameters, for our fiducial inclination i , as well as for $i + 5^\circ$ and $i - 5^\circ$. We find rotation velocities (V_{rot}) suggesting flat rotation curves for all our sample. For calculating V_{rot} , we use the mean velocity of the rings, as found with our fiducial inclination. The associated uncertainties come from the 16th and 84th percentiles of the velocity distribution obtained when considering the uncertainty in our inclination. To convert from V_{rot} to circular velocity (V_{circ}), we correct for pressure-supported motions using ${}^3\text{DBarolo}$ as well (see Iorio et al. 2017). As suggested by the narrowness of the PV diagrams (Figures 1 and 2), we find low velocity dispersions (P. E. Mancera Piña et al. 2019, in preparation), giving rise to very small asymmetric drift corrections ($\lesssim 2 \text{ km s}^{-1}$).

3. Results and Discussion

In Figure 3 we present the circular velocity–baryonic mass plane for our HI-rich UDGs, compared with galaxies from the SPARC (Lelli et al. 2016b), SHIELD (McNichols et al. 2016), and LITTLE THINGS (Iorio et al. 2017) samples. Clearly, all the UDGs studied here lie significantly above the BTFR.

Our galaxies rotate about 3 times more slowly than galaxies with comparable M_{bar} and effective radius (but higher surface brightness). Alternatively, they have about 10–100 times the M_{bar} of galaxies with similar V_{circ} (but smaller effective radius and higher surface brightness, on average). These low velocities are consistent with the observations by Leisman et al. (2017) and Janowiecki et al. (2019) of HI-rich UDGs having narrower W_{50} than galaxies of similar HI mass.

Before discussing the implications of this result we address its robustness. The baryonic masses here derived cannot be substantially overestimated: HI line fluxes can be measured with good accuracy (and we find fluxes in agreement with those derived from ALFALFA data by Leisman et al. 2017), and the distances to the galaxies in our sample ($\langle d \rangle \sim 90 \text{ Mpc}$) are large enough to be well represented by Hubble flow models, so the estimation of their HI mass is reliable. The HI-rich nature of our galaxies also implies that the stellar mass and its systematics play a rather minor role: even $M_\star = 0$ would not move the galaxies significantly in Figure 3.

A severe underestimation of the rotation velocities is also unlikely. First, the HI emission of the galaxies extends out to radii $\approx 8\text{--}18 \text{ kpc}$, and velocities obtained at such large radii are expected to be tracing the maximum of the rotation curve for any plausible dwarf galaxy dark matter halo (e.g., Oman et al. 2015, their Figure 2). Second, regarding the inclination correction, bringing the galaxies back to the BTFR would require a nearly face-on inclination ($i \approx 10^\circ\text{--}20^\circ$) for *all* of them, which is both unlikely and incompatible with the observed intensity maps, as illustrated in Figure 1, with an ellipse showing the inclination that the galaxy would need to be on the BTFR. Third, noncircular motions are not strong enough to solve the observed discrepancy: regardless of the mode(s), their order, phase, or amplitude, harmonic noncircular motions do not bias V_{rot} toward lower values systematically, as long as the viewing angle of the galaxy is random (Oman et al. 2019, their Figure 7), and the symmetry of the approaching and receding sides of our PV diagrams suggests the absence of anharmonic components. We also investigated with ${}^3\text{DBarolo}$ the presence of radial motions, but no clear evidence for this was found, although higher-resolution observations are needed to further confirm this.

¹¹ Version 1.4, <http://editeodoro.github.io/Bbarolo/>.

¹² Version 1.0.2, <http://github.com/kyleaoman/martini>.

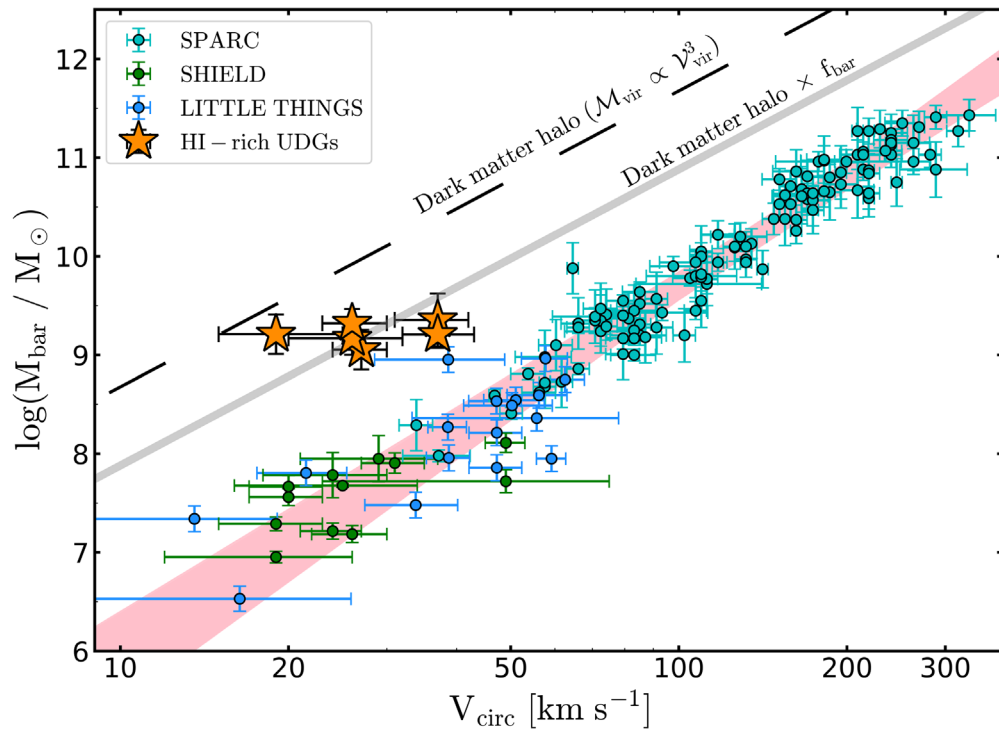


Figure 3. Circular velocity vs. baryonic mass plane. Galaxies from the SPARC, SHIELD, and LITTLE THINGS samples lie on top of the BTFR. The pink area is the 99% confidence interval of an orthogonal distance regression to the SPARC sample. HI-rich UDGs are clear outliers of the BTFR, and in a position consistent with having no “missing baryons.”

Finally, it is worth mentioning that the observed velocity gradients cannot be attributed to HI winds: in that case the gas velocity dispersion would be much higher than observed, and the galaxies would need very high star formation rate densities, opposite to what is measured (Leisman et al. 2017).

Previous studies already suggested the existence of outliers in the BTFR, or at least an increase in its scatter at low V_{circ} (e.g., Geha et al. 2006). Sometimes, however, the robustness of the measurements of the rotation velocities (usually estimated from the global HI profile) and inclinations of such outliers were unclear (see Oman et al. 2016 and references therein).

Based on the discussion above, we conclude that the positions of HI-rich UDGs in the $M_{\text{bar}} - V_{\text{circ}}$ plane derived here are robust, and our UDGs do not follow the BTFR.¹³ This suggests that the distribution of late-type systems in such a plane is broader than previously observed, and may have important implications for the scatter in the BTFR, which is a strong constraint for cosmological models. Despite the small scatter previously reported (e.g., Lelli et al. 2016a; Ponomareva et al. 2017), our findings open the possibility for a scenario where the parameter space in the $M_{\text{bar}} - V_{\text{circ}}$ plane between the UDGs presented here and the BTFR is populated by LSB galaxies whose resolved HI kinematics have not been studied yet, and which are not in our sample due to sharp selection effects. This may increase the error budget of the intrinsic scatter of the relation, but to properly understand the magnitude of this effect a more complete census of the relative abundances of these galaxies is required.

A second result emerges when comparing the position of our galaxies with the curves in Figure 3. The black dashed curve is

the relation between the circular velocity at the virial radius and the virial mass of dark matter halos ($M_{\text{vir}}/M_{\odot} \simeq 4.75 \times 10^5 (V_{\text{vir}}/\text{km s}^{-1})^3$, for $\Delta_c = 100$; see McGaugh 2012). If M_{vir} is multiplied by the cosmological baryon fraction ($f_{\text{bar}} \approx 0.16$), this gives rise to the solid gray curve, indicating the expected position for galaxies with a baryon fraction equal to f_{bar} .¹⁴ Unexpectedly, our UDGs lie on top of this curve, meaning that they are consistent with having no “missing baryons” within their virial radii.

Posti et al. (2019) recently discovered that some massive spirals have virtually no “missing baryons.” There is, however, a substantial difference between our UDGs and these massive spirals, as the former are HI-dominated and have very shallow potential wells compared to the latter. How, then, is it possible that they retained all of their gas? One intriguing possibility is that they have not experienced strong episodes of gas ejection: feedback processes must have been relatively weak and the shallow gravitational potentials managed to retain (or promptly reaccrete) all of their baryons. We surmise that this could be related to the low gas velocity dispersions we find for our sample, which suggest a currently weak heating of the gas. This may be analogous to the “failed feedback problem” of Posti et al. (2019), although in their case feedback has failed at limiting the star formation efficiency of massive spiral galaxies.

Extremely efficient feedback has been invoked to solve different discrepancies between observations and Λ CDM predictions (see Tulin & Yu 2018 and Bullock & Boylan-Kolchin 2017 for a review, including limitations of such solutions), as well as to explain the formation of UDGs via feedback-driven outflows resulting from bursty star formation

¹³ It is worth noting that the two outliers close to our UDGs, DDO 50 and UGC 7125, also have relatively large effective radii and/or low surface brightness.

¹⁴ Note that this assumes $V_{\text{circ}} \approx V_{\text{vir}}$, but in general V_{circ} tends to be slightly larger for massive galaxies ($V_{\text{circ}} \approx 1.5V_{\text{vir}}$). This would flatten the gray curve at high V_{circ} values.

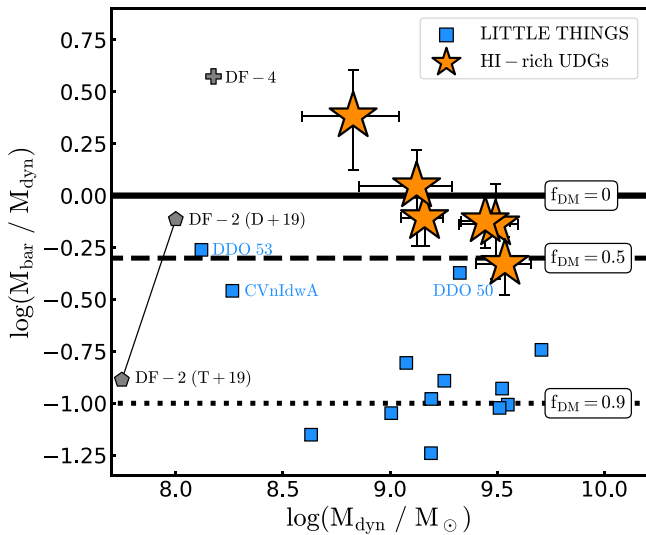


Figure 4. Baryonic to dynamical mass ratio as a function of the dynamical mass, measured inside $\approx 4 R_d$. The solid, dashed, and dotted lines show the position where galaxies with 0%, 50%, and 90% dark matter lie, respectively. LITTLE THINGS galaxies (Iorio et al. 2017) are shown for comparison, as well as two estimates for DF-2 (Danieli et al. 2019, D+19; Trujillo et al. 2019, T+19) and DF-4 (van Dokkum et al. 2019), for which we assume $M_{\text{bar}} = M_*$.

histories (e.g., Di Cintio et al. 2017). These new observations seem to present a challenge to these models.

An alternative scenario could be that our galaxies reside in halos with $V_{\text{circ}} \approx 80 \text{ km s}^{-1}$ but very low concentration, such that their rotation curves are still rising at our outermost measured radii. However, this does not seem feasible since the concentration parameter needed for this is $c \approx 1$, instead of the expected $c \approx 10$ (Ludlow et al. 2014), making the existence of such galaxies within the volume of the universe basically impossible.

Figure 4 shows the ratio between baryonic and dynamical mass of our UDGs, with the dynamical mass estimated as $M_{\text{dyn}}(<R_{\text{out}}) = V_{\text{circ}}^2 R_{\text{out}}/G$, with R_{out} the radius of the outermost point of the rotation curve. Both our sample and LITTLE THINGS galaxies have a mean $R_{\text{out}}/R_d \approx 4$, with R_d the optical disk-scale length.

Even if our HI-rich UDGs have a baryon fraction equal to the cosmological average, their dynamics could be dark-matter-dominated at all radii, as other galaxies of similar V_{circ} , but this does not seem to be the case, since $M_{\text{bar}}(R < R_{\text{out}}) \approx M_{\text{dyn}}(R < R_{\text{out}})$. Although more precise values of M_{bar} and M_{dyn} should be determined with better data, Figure 4 indicates that these galaxies have much less dark matter within the extent of their disks than other dwarfs and LSB galaxies, and that, inside their disks, the baryonic component dominates.

The dynamical properties shown here resemble those of tidal dwarf galaxies (Hunter et al. 2000, Lelli et al. 2015). However, given the isolation (mean distance to the nearest neighbor ~ 1 Mpc) of our UDGs, a tidal dwarf origin does not seem likely, but this is hard to test with the current data.

Based on their globular clusters kinematics the UDGs NGC1052-DF2 (van Dokkum et al. 2018; Danieli et al. 2019) and NGC1052-DF4 (van Dokkum et al. 2019) have recently been claimed to lack dark matter, although some concerns exist regarding their distances and environments (Monelli & Trujillo 2019; Trujillo et al. 2019). Our UDGs have robust distances determined from their recession velocities and avoid

dense environments, mitigating these concerns. They may be subject to different systematics, but demonstrate that there may indeed exist a previously underappreciated population of unusually dark-matter-deficient galaxies.

4. Conclusions

We have analyzed a set of interferometric HI line observations of gas-dominated UDGs. Using a 3D fitting technique we obtain robust measurements of their circular velocities, allowing us to place them in the circular velocity–baryonic mass plane.

We find that our six galaxies lie well above the BTFR, with rotation velocities too low given their baryonic masses. Their position in the circular velocity–baryonic mass plane implies that they have a baryon fraction within their virial radius equal or close to the cosmological value, and we speculate that this could be due to extremely inefficient feedback, challenging our current understanding of feedback processes in dwarfs. Additionally, the dynamics of these galaxies are dominated by the baryonic component out to the outermost measured radii, and they have very low dark matter fractions inside such radii, suggesting a broader distribution in the dark matter content of galaxies than previously thought.

The fact that galaxies with these properties had not been reported before is perhaps because interferometric HI observations are usually targeted based on previous optical studies. Since UDGs are an extremely optically faint population, it is not particularly surprising that this galaxy population has not been identified before. With the advent of large HI interferometric surveys we expect this hidden population to come to light.

We appreciate the careful revision and useful comments made by an anonymous referee. We thank Giuliano Iorio and Andrew McNichols for their clarifications on LITTLE THINGS and SHIELD data, respectively. We would also like to thank Anastasia Ponomareva, Arianna Di Cintio and Federico Lelli for interesting discussions.











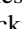




P.E.M.P. and F.F. are supported by the Netherlands Research School for Astronomy (Nederlandse Onderzoeksschool voor Astronomie, NOVA), Phase-5 research programme Network 1, Project 10.1.5.6. E.A.K.A. is supported by the WISE research programme, which is financed by the Netherlands Organization for Scientific Research (NWO). K.A.O. received support from VICI grant 016.130.338 of NWO. L.P. acknowledges support from the Centre National d’Études Spatiales (CNES). M.P.H. is supported by grants NSF/AST-1714828 and from the Brinson Foundation. This work has been supported in part by NSF grant AST-1625483 to K.L.R., and by The National Radio Astronomy Observatory (The National Radio Astronomy Observatory is a facility of the National Science Foundation operated under cooperative agreement by Associated Universities, Inc.). We have made an extensive use of SIMBAD and ADS services, for which we are thankful.

ORCID iDs

Pavel E. Mancera Piña <https://orcid.org/0000-0001-5175-939X>

Filippo Fraternali <https://orcid.org/0000-0002-0447-3230>

Elizabeth A. K. Adams <https://orcid.org/0000-0002-9798-5111>

Antonino Marasco  <https://orcid.org/0000-0002-5655-6054>
 Tom Oosterloo  <https://orcid.org/0000-0002-0616-6971>
 Kyle A. Oman  <https://orcid.org/0000-0001-9857-7788>
 Lukas Leisman  <https://orcid.org/0000-0001-8849-7987>
 Enrico M. di Teodoro  <https://orcid.org/0000-0003-4019-0673>
 Lorenzo Posti  <https://orcid.org/0000-0001-9072-5213>
 Michael Battapaglia  <https://orcid.org/0000-0002-3501-8396>
 John M. Cannon  <https://orcid.org/0000-0002-1821-7019>
 Lexi Gault  <https://orcid.org/0000-0002-2492-7973>
 Martha P. Haynes  <https://orcid.org/0000-0001-5334-5166>
 Steven Janowiecki  <https://orcid.org/0000-0001-9165-8905>
 Kameron Reiter  <https://orcid.org/0000-0001-8530-7543>
 Katherine L. Rhode  <https://orcid.org/0000-0001-8283-4591>
 John J. Salzer  <https://orcid.org/0000-0001-8483-603X>
 Nicholas J. Smith  <https://orcid.org/0000-0002-3222-2949>

References

- Bacchini, C., Fraternali, F., Iorio, G., & Pezzulli, G. 2019, *A&A*, **622**, 64
 Bullock, J. S., & Boylan-Kolchin, M. 2017, *ARA&A*, **55**, 343
 Dalcanton, J., Spergel, D. N., & Summers, F. J. 1997, *ApJ*, **482**, 659
 Danieli, S., van Dokkum, P., Conroy, C., Abraham, R., & Romanowsky, A. J. 2019, *ApJ*, **874**, 12
 de Blok, W. J. G. 1997, PhD thesis, Univ. Groningen
 den Heijer, M., Oosterloo, T. A., Serra, P., et al. 2015, *A&A*, **581**, A98
 Di Cintio, A., Brook, C. B., Dutton, A. A., et al. 2017, *MNRAS*, **466**, 1
 Di Cintio, A., Brook, C. B., Macciò, A. V., et al. 2019, *MNRAS*, **486**, 2535
 Di Teodoro, E., & Fraternali, F. 2015, *MNRAS*, **451**, 3021
 Di Teodoro, E. M., Fraternali, F., & Miller, S. H. 2016, *A&A*, **594**, A77
 Dutton, A. A. 2012, *MNRAS*, **424**, 3123
 Fattahi, A., Navarro, J. F., Sawala, T., et al. 2016, *MNRAS*, **457**, 844
 Geha, M., Blanton, M. R., Masjedi, M., & West, A. A. 2006, *ApJ*, **653**, 240
 Giovanelli, R., Haynes, M. P., Kent, B. R., et al. 2005, *AJ*, **130**, 2598
 Governato, F., Willman, B., Mayer, L., et al. 2007, *MNRAS*, **374**, 1479
 Herrmann, K. A., Hunter, D. A., Zhang, H.-X., & Elmegreen, B. G. 2016, *AJ*, **152**, 177
 Hunter, D. A., Hunsberger, S. D., & Roye, E. W. 2000, *ApJ*, **542**, 137
 Impey, C., Bothun, G., & Malin, D. 1988, *ApJ*, **330**, 634
 Iorio, G., Fraternali, F., Nipoti, C., et al. 2017, *MNRAS*, **466**, 4159
 Janowiecki, S., Jones, M. G., Leisman, L., et al. 2019, *MNRAS*, Advance Access, [stz1868](https://doi.org/10.1093/mnras/stz1868)
 Jones, M. G., Papastergis, E., Pandya, V., et al. 2018, *A&A*, **614**, 21
 Leisman, L., Haynes, M. P., Janowiecki, S., et al. 2017, *ApJ*, **842**, 13
 Lelli, F., Duc, P. A., Brinks, E., et al. 2015, *A&A*, **584**, A113
 Lelli, F., McGaugh, S. S., & Schombert, J. M. 2016a, *ApJ*, **816**, 14
 Lelli, F., McGaugh, S. S., & Schombert, J. M. 2016b, *AJ*, **152**, 157
 Ludlow, A. D., Navarro, J. F., Angulo, R. E., et al. 2014, *MNRAS*, **441**, 378
 Mancera Piña, P. E., Aguerri, J. A. L., Peletier, R. F., et al. 2019, *MNRAS*, **485**, 1036
 Mancera Piña, P. E., Peletier, R. F., Aguerri, J. A. L., et al. 2018, *MNRAS*, **481**, 4381
 Marasco, A., Fraternali, F., Posti, L., et al. 2019, *A&A*, **621**, 6
 McGaugh, S. S. 2005, *ApJ*, **632**, 859
 McGaugh, S. S. 2012, *AJ*, **143**, 40
 McGaugh, S. S., Schombert, J. M., Bothun, G. D., & de Blok, W. J. G. 2000, *ApJ*, **533**, 99
 McNichols, A. T., Teich, Y. G., Nims, E., et al. 2016, *ApJ*, **832**, 89
 Monelli, M., & Trujillo, I. 2019, *ApJ*, **880**, 11
 Oman, K., Marasco, A., Navarro, J. F., et al. 2019, *MNRAS*, **482**, 8210
 Oman, K., Navarro, J. F., Fattahi, A., et al. 2015, *MNRAS*, **452**, 3650
 Oman, K., Navarro, J. F., Sales, L. V., et al. 2016, *MNRAS*, **460**, 3610
 Ponomareva, A. A., Verheijen, M. A. W., Peletier, R. F., & Bosma, A. 2017, *MNRAS*, **469**, 2387
 Posti, L., Fraternali, F., & Marasco, A. 2019, *A&A*, **626**, 56
 Román, J., & Trujillo, I. 2017, *MNRAS*, **468**, 4039
 Sales, L. V., Navarro, J. F., Oman, K., et al. 2017, *MNRAS*, **464**, 2419
 Sandage, A., & Binggeli, B. 1984, *AJ*, **89**, 919
 Sawala, T., Frenk, C. S., Fattahi, A., et al. 2016, *MNRAS*, **457**, 1931
 Trujillo, I., Beasley, M. A., Borlaff, A., et al. 2019, *MNRAS*, **486**, 1192
 Tulin, S., & Yu, H.-B. 2018, *PhR*, **730**, 1
 van Dokkum, P. G., Abraham, R., Merritt, A., et al. 2015, *ApJL*, **798**, L45
 van Dokkum, P., Danieli, S., Abraham, R., Conroy, C., & Romanowsky, A. J. 2019, *ApJL*, **874**, 5
 van Dokkum, P., Danieli, S., Cohen, Y., et al. 2018, *Natur*, **555**, 629
 Vogelaar, M. G. R., & Terlouw, J. P. 2001, in ASP Conf. Ser. 238 *Astronomical Data Analysis Software and Systems X*, ed. F. R. Harnden, Jr, F. A. Primini, & H. E. Payne (San Francisco, CA: ASP), 358
 Zwaan, M., van der Hulst, J., de Blok, W., & McGaugh, S. 1995, *MNRAS*, **273**, L35